CHALMERS
UNIVERSITY OF TECHNOLOGY

Development of a ship performance model for power estimation of inland waterway vessels

Ocean Engineering 287 (2023) 115731

Contents lists available at ScienceDirect

Ocean Engineering

journal homepage: www.elsevier.com/locate/oceaneng

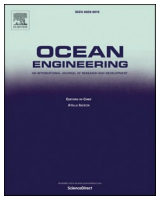

Development of a ship performance model for power estimation of inland waterway vessels

Chengqian Zhang *, Jonas W. Ringsberg, Fabian Thies

Chalmers University of Technology, Department of Mechanics and Maritime Sciences, Division of Marine Technology, SE-412 96, Gothenburg, Sweden

ARTICLE INFO

Handling Editor: Prof. A.I. Incecik

Keywords:
Energy efficiency
Inland waterways
Ship performance model

ABSTRACT

A ship performance model is an important factor in energy-efficient navigation. It formulates a speed–power relationship that can be used to adjust the engine loads for dynamic energy optimisation. However, currently available models have been developed for sea-going vessels, where the environmental conditions are significantly different from those experienced on inland waterways. Inland waterway shipping has great potential to become a mode of transport that can both improve safety and reduce emissions. Therefore, this paper presents the development of an energy performance model specifically for inland waterway vessels (IWVs). The holistic ship energy system model is based on empirical methods, from resistance to engine performance prediction, established in a modular code architecture. The resistance and propulsion prediction in confined waterways are captured by a newly developed method, considering a superposing of shallow water and bank effect. Verification against model tests and high-fidelity simulations indicate that the selected empirical methods achieved good accuracy for predicting ship performance. The resistance prediction error was 5.2% for single vessels and 8% for pusher-barge convoys based on empirical methods. The results of a case study investigating the performance of a self-propelled vessel under dynamic waterway data, indicate that the developed model could be used for onboard power monitoring and energy optimisation during operation.

1. Introduction

The transport sector accounts for a significant part of Europe's greenhouse gas emissions (Eurostat, 2023),with road transportation comprising a dominant part of the European Union's freight shipping network for the past few decades. With increased restrictions on emissions and congestion on the roads, a practical solution must be found to ease the pressure on road-based transportation in an efficient and sustainable manner. One solution with significant potential involves European inland waterways, which have a total length of over 40,000 km and connect hundreds of major cities and ports. Nevertheless, these rivers and canals have been underused for goods transportation during recent decades. Compared to other transport modes, inland waterways comprise only 6% of the EU's inland freight transport (Eurostat, 2022).

A shift from road-based to inland waterway transportation would result in more energy-efficient transportation and reduced emissions. The increased use of inland waterways should, however, be planned to meet future expectations and demands for sustainable, efficient, and reliable modes of transport. Fossil-free transport options with a high degree of automation or autonomy are considered as future solutions. The EU-funded project AUTOBarge (European Commission, 2020), which is studying these issues, aims to build a smart waterborne transportation network by utilising autonomous inland vessels for intelligent shipping. Thus, it needs numerical simulation models to capture and analyse different inland waterway vessels' (IWVs) characteristics and performance, to determine whether new designs are needed and how they should be safely operated, navigated, and routed. Such a model should include a vessel power prediction tool, a manoeuvring model and a routing or voyage planning model.

Existing ship performance models have been developed for sea-going vessels, where the environmental inputs are different from those experienced on inland waterways. The current study presents the development of a new power prediction model specifically developed for inland vessels. To improve the competitiveness of inland shipping regarding energy efficiency and emissions reduction, an accurate estimation of energy consumption with computational efficiency is a critical factor. A ship performance model provides an effective method of simulating and studying a ship's energy system by considering the desired sailing speed and the interaction with dynamic water conditions, the so-called speed–power relationship.

* Corresponding author.
E-mail address: chengqian.zhang@chalmers.se (C. Zhang).

https://doi.org/10.1016/j.oceaneng.2023.115731
Received 19 April 2023; Received in revised form 17 August 2023; Accepted 27 August 2023
Available online 14 September 2023

Nomenclature

A_{WP}	Ship waterplane area [m^2]
B	Ship beam [m]
C	Duct chord length [m]
C_B	Block coefficient [-]
C_F	Frictional resistance coefficient [-]
CFD	Computational fluid dynamics
C_W	Wave resistance coefficient [-]
D	Propeller diameter [m]
d	Distance between vessel and bank [m]
DoF	Degree of freedom [-]
ETA	Estimated time of arrival [h]
FC_{obj}	Objective function of fuel consumption
Fr_h	Depth Froude Number [-]
Fr_{hd}	Depth Froude Number (deep water) [-]
H	Water depth [m]
IWV	Inland waterway vessel [-]
k	Ship form factor [-]
L	Ship length overall [m]
n_{Prop}	Number of propellers [-]
P_D	Delivered power [kW]
P_E	Effective power [kW]
P_S	Service power [kW]
P_{max}	Engine limits [kW]
Q	River discharge rate [m^3/s]
R_{AW}	Added wave resistance [kN]
R_{BANK}	Bank-induced resistance [kN]
R_s	Squat-induced resistance [kN]
R_T	Total resistance [kN]
R_W	Wind resistance [kN]
$SFOC$	Specific fuel oil consumption [g/kWh]
S_W	Wetted surface area [m^2]
T	Ship draft [m]
t	Thrust deduction factor [-]
UKC	Under keel clearance [m]
Vs	Ship speed [km/h]
U_C	Speed of currents [m/s]
W_C	River channel width [m]
w_E	Effective wake [-]
y_{infl}	Influence distance of bank effect [m]
η_H	Hull efficiency [-]
η_o	Propeller open water efficiency [-]
η_R	Relative rotative efficiency [-]
η_s	Shaft transmission efficiency [-]
ρ_{FW}	Fresh water density [kg/m^3]
ρ_{SW}	Sea water density [kg/m^3]
τ	Propeller thrust ratio [-]

1.1. Categories of ship performance models for open water conditions

The currently available ship performance models discussed in the literature can be divided into two types: (i) white box models, which consider the physics and engineering properties of the ship, and (ii) black box models (or data-driven machine learning models), which utilise large amounts of field data from measuring ship parameters and environmental inputs to build a regression model to predict energy consumption during dynamic operation.

Regarding the performance of ship energy systems-based models (white box models), active research has been focusing on conventional ocean-going vessels. Calleya (2014) developed the Ship Impact Model (SIM) for the quick prediction of standard commercial ships' energy performance with different techniques for reducing carbon during the early design stage. Lu et al. (2015) designed a semi-empirical performance prediction model which aims to estimate ship fuel consumption at corresponding sea states and encounter angles. Tillig et al. (2017) proposed a holistic ship energy performance model that can systematically estimate a ship's energy consumption by integrating sub-models that represent the key parameters of the entire energy system. The model can either be used in the early design phase for energy prediction with limited input or for analysing the performance of existing vessels using detailed hull parameters and environmental data. Similarly, Huang et al. (2021) developed a whole ship model with an extended method for ice resistance estimation, enabling the use of the model for ships travelling Arctic routes.

In addition to these empirical formula-based models, several data-driven models, based on ample measured data from different ship hull types and journeys, have also been developed in recent years to predict ship performance (Hu et al., 2019; Karagiannidis and Themelis, 2021; Lang et al., 2022; Parkes et al., 2018). Gupta et al. (2022) proposed a machine learning (ML) method to predict the hydrodynamic performance of commercial vessels using collected service data. Bui and Perera (2021) developed an ML-based framework to quantify the best ship performance under local operational conditions, such as trim-draft and corresponding engine modes. Yuan et al. (2021) proposed a data-driven model for predicting the instant ship fuel consumption based on data collection from various onboard sensors, and a heuristic optimisation algorithm was utilised to optimise the engine speed for reducing fuel consumption. In these black box models, researchers established training sets from full-scale trial data and considering the impact of parameters such as hull form, sailing speed, weather input and engine limits. These prediction models have demonstrated good generalisation ability, allowing for their onboard adaptation as a rapid prediction tool during navigation.

1.2. Performance models for inland waterways vs open water

In general, there are many available ship performance models that work well for ships on open water. However, the sailing conditions on inland waterways differ considerably from those on open waters. As an example, the confinement effect of waterways significantly impacts a ship's propulsion power. Further, course keeping and manoeuvring is more important on inland waterways due to the constrained space of rivers and canals. Consequently, the models developed for sea-going vessels become less applicable on confined waterways as they do not consider the shallow water and bank effect but focus instead on the added resistance from wind and waves, which are less significant on inland waterways.

For a ship sailing on inland waterways, the decreased water depth and confinement due to channel geometry can have a significant impact on the flow field around the ship. The accelerated water around the ship's hull leads to a sinkage and trim of the vessel and thus increase hydrodynamic forces. Therefore, an accurate prediction of shallow water resistance and propulsive factors is critical for power estimation and computation of energy consumption. Several empirical models have been proposed for the prediction of inland water resistance based on experimental results (Aztjushkov, 1968; Geerts et al., 2010; Karpov, 1946; Landweber, 1939; Schlichting, 1934). Such methods use empirical formulas for deep water resistance and include a speed correction in shallow water. However, Raven (2016) investigated these methods and uncovered their various shortcomings due to their lack of a physical basis and oversimplification of the problem in real inland water scenarios. In addition, these formulas were derived based on data from

conventional sea-going vessels, whose hull forms are distinctive from inland vessels; thus, the formulas become less applicable when used for rivers and canals.

In recent years, an increasing number of model tests have been conducted to collect benchmark data with a special focus on inland vessels (Friedhoff et al., 2019; Mucha et al., 2017, 2018; Zeng et al., 2018). Friedhoff et al. (2019) conducted an experiment using a Particle Image Velocimetry (PIV) test to investigate the effect of water depth on the wake fraction of a large Rhine vessel in different stern shapes. In addition, Zentari et al. (2022) conducted systematic model tests to investigate the resistance and propulsion of different arrangements of pusher-barge convoys to study the confinement effect on inland vessels.

Along with the model test development for inland vessels, research over the past decade has used computational fluid dynamics (CFD) to investigate the effect of restricted waterways. Extensive studies (Du et al., 2020; Islam et al., 2021; Linde et al., 2017; Zeng et al., 2019; Zou and Larsson, 2013) have been performed to predict resistance and propulsive factors in shallow or confined waterways. Campbell et al. (2022) utilised the RANS-based CFD method to investigate the influence of changing trim and squat on total resistance on confined waterways, followed by a study on dynamic trim optimisation and the effect of various sailing speeds. In addition, Du et al. (2021) analysed the unsteady hydrodynamic behaviour of a pushed convoy passing bridge piers, and their computation of resistance squat and ship-generated waves from CFD showed good agreement with their experimental results. With the help of mature simulation methods and computing power, CFD can accurately predict hull forces for a ship on confined waterways. However, both model tests and CFD simulations can only predict a single operating condition (single water depth condition, constant ship speed for a specific hull form) during each trial. The inland vessels may encounter dynamic conditions in actual operation, such as varying water depth, river width, current angle, and speed. Therefore, the solution needs to build a regression model that considers the effects of changing these parameters to cover real sailing conditions. However, this approach requires numerous trials, which can be expensive and time-consuming, and when the vessel type changes, the model may become less applicable.

1.3. Objective and outline of the study

Regarding the power prediction methods for inland vessels, most existing research focuses on the hydrodynamics of a particular ship type in shallow or fully confined waterways (see, e.g., Du et al., 2020; Islam et al., 2021; Linde et al., 2017). In contrast, the propeller and the engine normally use simple equations with constant propulsion coefficients. Besides, these methods are limited to a specific vessel type and thus lack of applicability for generic application.

To the authors' knowledge, there is no currently available study that has developed a physics-based (White box) model for the performance prediction of IWVs including the holistic energy system (combining hull, propeller, and engine model). Therefore, this study presents a new generic ship performance model for IWVs. It is computationally efficient (rapid) with acceptable accuracy and only requires limited input parameters to model a vessel and simulate a voyage. Thus, it can be used for multiple scenario simulations and Monte Carlo simulations to assess energy consumption, compare operating conditions, and consider dynamic/optimised route planning, for example.

The model is an extensive development of the ship energy prediction model ShipCLEAN (Tillig and Ringsberg, 2019), which was originally developed for sea-going vessels. Due to the different characteristics of inland vessels and sea-going ships, the new model presented in this study has incorporated many changes to the major modules of the ShipCLEAN model, such as ship hull modelling, resistance prediction, propeller design and power prediction. Hence, it includes all the factors needed for a IWV to represent its energy system and hydrodynamics. The study performed and presented a validation against model tests on different inland vessel types to investigate prediction accuracy.

The remainder of this article is organised as follows: Section 2 outlines the energy performance model and identifies the major challenges for ship performance prediction in inland waterways. Subsequently, Section 3 presents an overview of the new model, called ShipCLEAN-IWV, including a detailed discussion of each sub module, which also presents the important factors for the entire energy system. After that, Section 4 demonstrates the simulation and validation against the model tests, followed by case studies of single vessels and pushed convoys with different loading conditions to analyse energy consumption during operation. Finally, Section 5 summarises the development of the model and presents the conclusions of the study.

2. Holistic ship energy system modelling

The new ShipCLEAN-IWV model presented in this study is an extension and modification of the ShipCLEAN model developed by Tillig and Ringsberg (2019). Section 2.1 gives a short presentation of the original ShipCLEAN model, Section 2.2 highlights new features that have been modelled in the new ShipCLEAN-IWV model, followed by Section 2.3 that the presents applicability of the new model.

2.1. ShipCLEAN for sea-going vessels

ShipCLEAN was originally designed for commercial vessels on open water. The model follows a modular concept of a ship's energy system, in which each module represents a critical component of the entire ship for energy systems analysis, such as the hull form, resistance prediction, propeller, engine modelling and units for wind-assisted ship propulsion. The model development process can be found in detail in Tillig et al. (2017, 2018) and Tillig and Ringsberg (2020). One advantage of such modular-based architecture is that modules can be modified or added depending on their purpose within the ship's energy system. The ShipCLEAN model consists of two major parts, one for static power prediction called ShipPOWER and the other for dynamic operation with routing and weather data called ShipJOURNEY.

The overall objective of the generic ship energy model is to use limited input parameters to perform power predictions and energy consumption estimations. During the early design stage in particular, the geometry and detailed hull form data are normally unavailable. As a result, ShipPOWER uses basic parameters such as ship type, main dimensions (length, beam, draft, displacement), propeller arrangement with rpm, and design speed to estimate static power and energy consumption using a combination of empirical formulas and interpolation methods. Since it is based on empirical approaches, the computational time is quite short compared to CFD simulation. Moreover, the model considers various kinds of ships, and its input parameters can be easily modified to represent a specific vessel type. The output of ShipPOWER includes.

(i) hull form, based on standard series with remaining dimension parameters such as wetted surface and superstructure,
(ii) resistance curve in calm water,
(iii) power prediction based on sea states and wind,
(iv) propeller properties,
(v) engine performance with energy consumption prediction, and
(vi) linear hydrodynamic parameters.

These predictions become a critical input for the second part of the model, ShipJOURNEY, which focuses on the dynamic prediction of ship energy performance during operation. The input parameters consist of the output from ShipPOWER, routing data, weather information and operation conditions, such as loading rate, design speed and sailing mode (e.g., constant speed, constant power, estimated time of arrival (ETA)). ShipPOWER estimates the power demand, energy consumption, speed and ship attitude (yaw and heel angle) at each waypoint in the

route to predict the ship's performance during dynamic operations.

ShipCLEAN was validated against model tests and full-scale measurements for different ship types, and the results showed good agreement between the model's predictions and actual measurements (Tillig, 2020).

2.2. ShipCLEAN-IWV for inland waterway vessels

The empirical methods in ShipCLEAN were selected for conventional sea-going vessels, for which the effects of shallow and confined waterways were not considered. Many researchers have confirmed that such effects are critical for resistance prediction and power estimation on confined waterways and must be included in a model for IWVs (Kulczyk, 1995; Millward, 1989; Mucha et al., 2018; Raven, 2016). Additionally, the sailing conditions for IWVs differ significantly from open water conditions. Moreover, the properties of IWVs (hull type, propulsion units, rudder arrangement and engine parameters) differ from those of ships sailing in open water. Therefore, based on the modular architecture of the original ShipCLEAN, this study proposed a new model aiming at capturing the characteristics of IWVs, which is called ShipCLEAN-IWV.

Like the original model, the objective, and characteristics of the ShipCLEAN-IWV developed in this study are to propose a simulation model that enables performing a fast and accurate prediction on propulsion power and energy consumption for inland vessels. Therefore, the model utilises a modular architecture and is developed based purely on empirical methods.

For the resistance prediction module, this model includes the effect of changing water depth by an integration of empirical methods in shallow water, and the results were validated against experimental data. In addition to the shallow water resistance, the model also includes an estimation of the bank effect from a collection of publicly available model test results. To give an accurate prediction on propeller efficiency for IWVs, the study modified the previous propeller module using the blade section details of classical inland propellers and incorporated a duct design. Besides, the engine module was proposed from a regression analysis of diesel engines with different power range. The development of these modules, modification of empirical formulas and methods used are presented in Section 3 in detail.

2.3. Applicability and limitations of the model

The model was designed for conventional IWVs on European inland waterways, such as tankers, container ships and self-propelled barges. Therefore, the propulsion system modelling only considers commonly used devices (such as screws or ducted propellers and diesel/gas engines). As a result, the model mainly focuses on classical vessel types, propulsion units and engine systems. Novel equipment, such as waterjets, electrical engines, and hybrid engines, are not included in this paper.

For the bank-effect estimation, the channel wall is assumed to be vertical, and thus the impact of detailed parameters, such as bank slope and geometries, are not included in the present study. Moreover, since the model was designed for normal sailing conditions on inland waterways, the ship's hydrodynamic behaviour while crossing locks and bridge piers is out of scope. In addition, the current model does not include the effects of neighbouring ships passing the target ship at close distance, which may affect the resistance or manoeuvrability of the target ship.

3. Performance model ShipCLEAN-IWV

3.1. Model overview

Fig. 1 presents the overall structure of the developed model. The simulation input parameters include vessel dimensions, propeller characteristics, engine limit and the desired operational water depth. The model output includes the prediction of the propulsion power and energy consumption under dynamic conditions encountered on inland waterways, including speed of the river currents U_C and varying water depth.

The major components of the ShipCLEAN-IWV energy system model are represented by the following modules: i) the geometry estimation calculates the wetted surface area and superstructure dimensions from the basic model's input; if the studied vessel's details are available, the module output can be easily replaced by the actual ship wetted surface and wind resistance coefficient; ii) resistance prediction represents a critical factor which includes the confinement effect of inland waterways; iii) the propulsive factors consider the effective wake and thrust deduction including effects from the varying water depth, and the results become important factors in the subsequent propeller design; iv) the propeller is modelled using OpenProp with blade section details of commonly used ducted propellers for inland ships; this module aims at providing detailed propeller open water curves rather than using equations only to determine propeller efficiency; v) the engine model can predict fuel oil consumption based on the model's inputs and results from previous modules; and vi) the dynamic operational analysis uses a defined route with water depth, bank width and current speed at each waypoint for the total fuel consumption calculation. The following subchapters describe how these modules were developed or revised

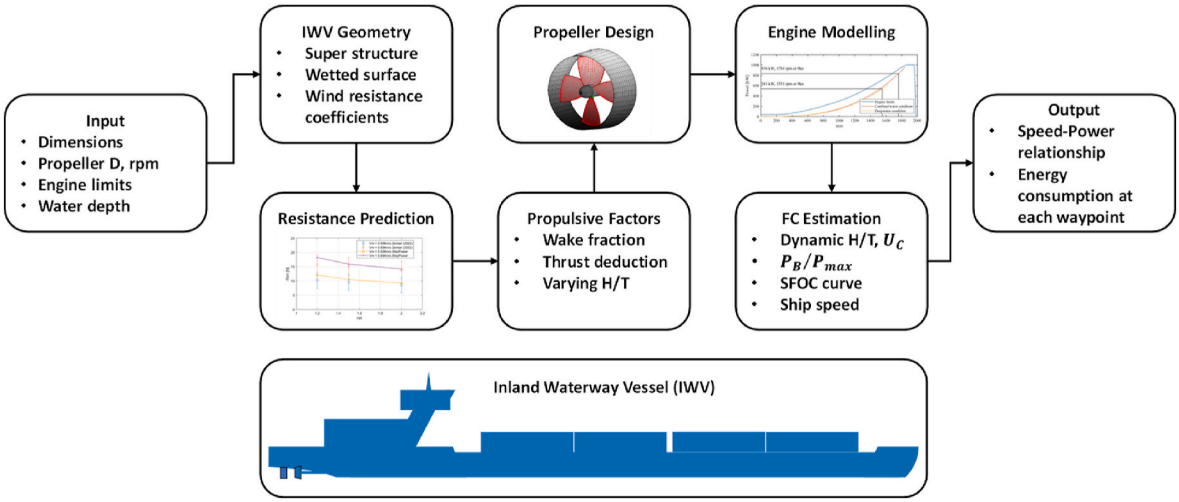

Fig. 1. Overview of the ship performance model ShipCLEAN-IWV.

based on the modules in ShipCLEAN (Tillig, 2020).

3.2. Process and units for performance prediction

3.2.1. Resistance prediction with confinement effect

Resistance prediction is a critical part of the energy system model since the estimated total resistance R_T has a direct impact on the demand power prediction as well as the energy consumption results. In the original ShipCLEAN model, the resistance formula in open sea water is given as:

$$R_T = 0.5\rho_{SW} V_S{}^2 S_W((1+k)C_F + C_R) + R_W + R_{AW} \quad (1)$$

where ρ_{SW} is the density of sea water, V_s is the ship speed, S_W is the wetted surface area, k is the form factor, C_F is the frictional resistance coefficient, C_R is the residual resistance coefficient, R_W is the added wind resistance and R_{AW} is the added wave resistance, respectively. Nevertheless, the sailing environment of inland waterways is significantly different from open water conditions, an inland vessel might not encounter ocean waves and rarely suffer from strong wind during daily operation (Pompée, 2015). Therefore, the ShipCLEAN-IWV mainly focuses on the modification of the left term (calm water resistance) as the confinement effect (e.g., shallow water and bank effect) can have huge impact on the static power prediction. As shown in Fig. 1, the function for wind resistance prediction is remained in the current model but will be neglected during the simulation unless field measured wind data is available. Previous studies (Linde et al., 2017; Raven, 2012, 2016) proved that conventional speed correction methods in shallow water involve significant limitations due to a lack of physical basis and over-simplification. Therefore, this study developed a new resistance prediction module that includes the shallow water and bank effect to capture the characteristics of inland waterways.

Raven (2016) showed that the corrections for shallow water should focus on the relationship between viscous resistance and water depth ratio ($\frac{H}{T}$) in addition to a speed correction. A comparison of model test data demonstrated that the results represent a significant improvement over the conventional methods. However, this method only works for $\frac{H}{T} > 2.0$ (where H is the water depth and T is the ship draft), and the ship types are mostly sea-going vessels. Zeng et al. (2019) subsequently proposed an improved method for shallow water resistance prediction. It is divided into the estimation of frictional resistance C_F, form factor k and wave-making resistance C_W with the effect of $\frac{H}{T}$ and the functions of hull forms; this method is especially useful for extremely shallow water conditions (i.e., $\frac{H}{T} = 1.2$). Since IWVs normally sail at relatively low speeds, this study utilises the method from Zeng et al. (2019) only for viscous resistance correction, and C_W remains the same in deep water. Moreover, estimating k in shallow water requires detailed parameters and is sensitive to specific ship types. Therefore, to make the model work for a wide range of inland vessels, this study only uses Zeng et al. (2019) formula for deep water k estimation and incorporates the more generic method proposed by Millward (1989) for form factor correction.

Total resistance in the model is formulated as:

$$R_T = 0.5\rho_{FW} V_S{}^2 S_W C_T + R_S + R_{BANK} \quad (2)$$

where ρ_{FW} is the freshwater density, V_S is the ship's speed, S_W is the wetted surface area, R_S is the additional resistance due to squat in shallow water, R_{BANK} is the additional resistance due to bank effect, and C_T is the total resistance coefficient, which is computed as follows:

$$C_T = \left(1 + \left(k_{deep} + \triangle k\right)\right)C_F^* + C_W \quad (3)$$

where k_{deep} is the form factor in deep water, Δ_k is the form factor correction to shallow water from Millward (1989), and C_F^* is the frictional resistance with the effect of water depth. The Δ_k and C_F^* are given as:

$$\triangle k = 0.644\left(\frac{H}{T}\right)^{-1.72} \quad (4)$$

$$C_F^* = \frac{0.08468}{(\log_{10}Re - 1.631)^2}\left(1 + \frac{c_1}{\log_{10}Re + c_2}\left(\frac{H}{T}\right)^{c_3}\right) \quad (5)$$

where c_1, c_2 and c_3 are determined by ship type. Zeng's (2019) study investigated three types of ships with different hull fullness, and Table 1 lists these parameters in detail, among them the Rhine Ship 86, is a typical inland vessel and its parameters are thus selected as the baseline for the simulations in this study. In contrast to the ITTC correlation lines, the frictional resistance depends not only on Re but also on hull type and $\frac{H}{T}$. Zentari et al. (2022) also concluded that C_F increases when the water depth decreases, especially when $\frac{H}{T} \leq 2.0$, thus indicating that the conventional ITTC method might underestimate frictional resistance in shallow water. For the vessels whose hull shapes differ from the reference significantly, a "virtual ship method" is utilised to include the effect of shape changes on resistance, as shown in Fig. 2. The draft of the virtual ship is represented by T_e, which is computed by:

$$T_e = \gamma T \quad (6)$$

where the γ is the equivalent factor, which indicates the fullness of hull (see Appendix A).

The effect of dynamic sinkage is also considered in the prediction of resistance. Raven (2016) proposed a sinkage prediction method based on ship fullness and depth Froude Number Fr_h, given as:

$$\Delta_{sinkage} \Big/ L = c_z \frac{\nabla}{L^3}\left[\frac{Fr_h{}^2}{\sqrt{1 - Fr_h{}^2}} - \frac{Fr_{hd}{}^2}{\sqrt{1 - Fr_{hd}{}^2}}\right] \quad (7)$$

where c_z is a coefficient depending on hull fullness with an average value of 1.46 (Hooft, 1977), and $Fr_{hd} = \frac{V_S}{\sqrt{0.3gL}}$ is the depth Froude Number in deep water. Therefore, the sinkage-induced resistance is computed as follows:

$$R_S \,/\, R_T = \left(\Delta_{sinkage} A_{WP} \big/ \nabla\right)^{2/3} \quad (8)$$

This equation suggests that the sinkage results in an increased wetted surface area and, correspondingly, an increased hull resistance.

In addition to the shallow water effect, the hull resistance can also be affected by the presence of banks in inland waterways. Lataire et al. (2009) proposed a mathematical model for predicting the bank effect based on systematic model tests, which use an influence distance y_{infl} to determine the effective region for bank-induced force. If the distance between the ship and the bank exceeds this value, no significant bank effect is found on the hull forces and moments. The y_{infl} is given as:

$$y_{infl} = 5B(Fr_h + 1) \quad (9)$$

Further experiments and simulations concluded that resistance only increases significantly if the ship is close enough to the bank wall. Mucha et al. (2018) and Du et al. (2020) similarly observed that an obvious resistance change occurs when the ship wall distance d decreases from approximately 2.5 B to 1.0 B, where B is the beam of vessel. Therefore, this study considered that strong bank effects would occur within this region; and the bank wall distances of less than 1.0 B is not considered in this paper due to the extreme difficulty and high uncertainty involved in this additional resistance prediction. The study assumed the channel to

Table 1
Constants c_1, c_2 and c_3 for different ship types (Zeng et al., 2019).

Vessel	C_B	c_1	c_2	c_3
Wigley hull	0.445	0.3466	−0.4909	−1.461
KCS	0.651	1.2050	−0.5406	−1.451
Rhine Ship 86	0.860	1.1680	−0.5238	−1.472

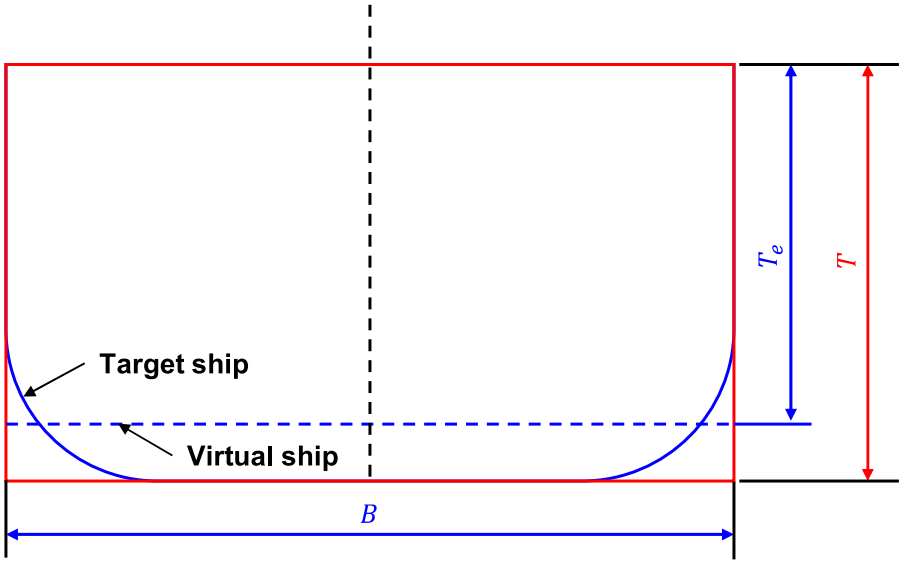

Fig. 2. Equivalent draft T_e of the virtual ship, reproduced from Zeng (2019).

be rectangular with a flat bottom and vertical wall, as shown in Fig. 3.

The results of the bank-induced effects from Linde et al. (2017), Mucha et al. (2018) and Du et al. (2020) (see Appendix B) are summarised in Fig. 4. The figure shows that R_{BANK} is affected by Fr_h and relative ratio of ship-bank distance and beam (d/B); if the ship sails at high speed close enough to the channel wall, the additional resistance can reach 30%. Based on the experimental measurements, R_{BANK} can be interpolated based on ship speed, position in the channel, and encountered water depth data collected during dynamic operation. According to the experimental data in the aforementioned literature, the applicable range for the total resisatance prediction is Fr_h varies from 0.1 to 0.75, which covers the typical speed range of inland vessels.

3.2.2. *Propeller design and propulsive factors*

The propeller design is based on a parametric standard series defined in OpenProp (Epps et al., 2009), if detailed geometry data is unavailable during the early design stage. Due to waterway restrictions, ducted propellers with nozzles are commonly used on inland ships to improve the efficiency of propellers with a limited diameter. Therefore, this study utilises the most used Ka-series propellers with nozzles to analyse the performance of the propulsion units.

OpenProp uses basic input data, such as propeller diameter, disc

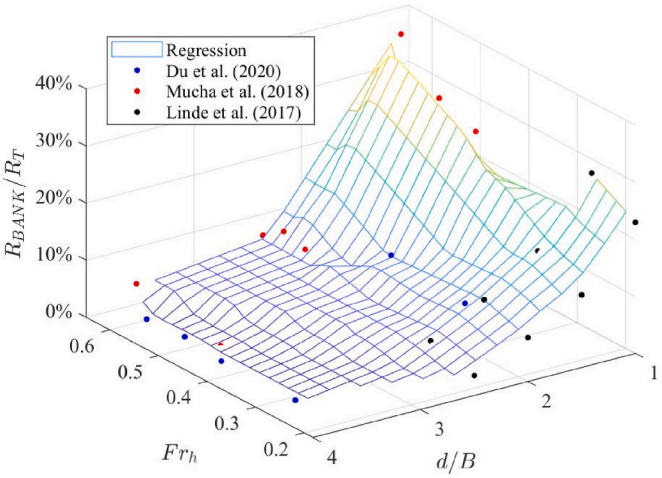

Fig. 4. Experimental and simulation data from Linde et al. (2017), Mucha et al. (2018) and Du et al. (2020).

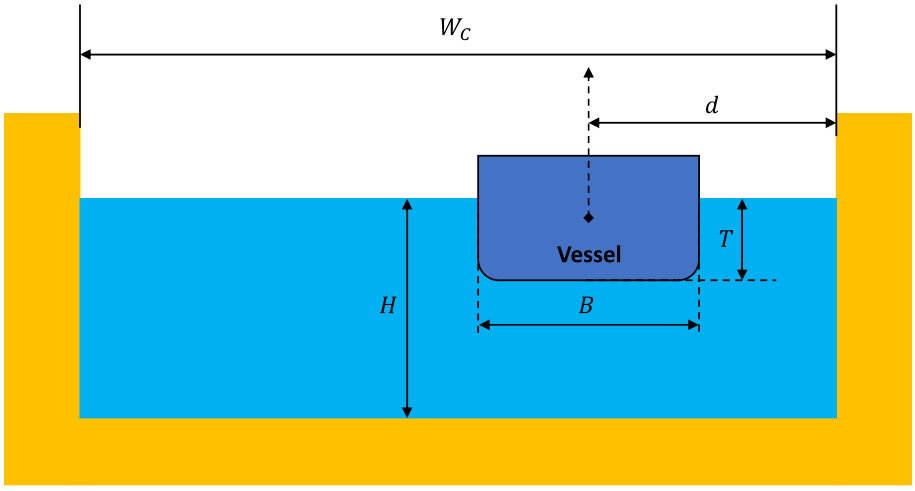

Fig. 3. Channel cross section of the rectangular fairway used in this study.

ratio and chord length at each blade section, as well as duct dimensions for the propeller design and performance estimation. The propeller thrust is computed from the resistance results divided by the number of the propellers (n_{Prop}), and the propeller open water efficiency curve is generated accordingly, which can be used to the dynamic power prediction.

In terms of the propulsive factors, effective wake fraction (w_E) and thrust deduction factor (t) in inland waterways become difficult to predict since most of the empirical methods were designed for open water and do not include the interaction between hull and waterway bottom. Model tests that include wake measurements in shallow water are relatively few among the existing studies. The decreasing water depth affects the flow field in the vicinity of the propellers, and stronger flow separation may contribute to higher wake and thrust deduction in limited water depths (Friedhoff et al., 2019; Kulczyk, 1995; Kulczyk and Tabaczek, 2014; Rotteveel et al., 2017). Kulczyk (1995) indicated that the difference between nominal wake and effective wake becomes obvious in shallow water because the working propeller can suppress the flow separation. Moreover, an accurate prediction of the thrust deduction depends on the stern geometry and the position of the propeller and the rudder. Conventional methods, such as those used by Harvald (1992), do not include the effect of water depth and stern tunnel and thus may provide an incorrect estimation in inland waterways. Therefore, to avoid overestimating the propulsive coefficients and to achieve an accurate power prediction, this study used the w_E and t from the model test by Kulczyk and Tabaczek (2014), who designed their experiment for inland ships with stern tunnels under different speeds and water depths. Table 2 lists the values of these coefficients in detail. The demand service power (P_S) can be computed using:

$$P_S = \frac{R_T V_S}{\eta_H \eta_O \eta_R \eta_S} \tag{10}$$

where P_s is the propulsion power output of the engine, η_H is the hull efficiency ($\eta_H = 1 - t/1 - w_E$), η_O is the propeller open water efficiency, η_R is the relative rotative efficiency, set to 1.0 in the current study, and η_S is the transmission efficiency including the combination of gear box and shaft loss, which is 0.97 in this study.

3.2.3. Engine modelling

Based on the power prediction at the design speed, an engine module was developed according to the dynamic fuel consumption estimation. This study adopts the engine MAN D2862 as a reference type, which is a commonly used four-stroke diesel engine for inland commercial vessels. According to the engine model, the instant fuel consumption can be derived by the ratio between P_S and engine limits from the specific fuel oil consumption (*SFOC*) curve, as shown in Fig. 5.

Apart from using the actual *SFOC* curve for the specific engine type, this study also includes method to predict engine performance. Especially during the early design stage, the exact engine type is generally unknown due to the limited available parameters. Therefore, the design propulsion power is typically the only input. Under such conditions, the highest value of power P_{max} is determined by the R_T under the shallowest water depth ($\frac{H}{T} = 1.2$) at the design speed and corresponding propulsive coefficients from the open water curve. The *SFOC* prediction is based on a mathematical model from Hidouche et al. (2015), which used a single input parameter (power ratio P_S/P_{max}) for the *SFOC* calculation. The regression analysis was conducted using *SFOC* data from marine engine manufactures, such as Cummins, MAN, Caterpillar and Wärtsilä, with various power ranges. The equations of the model can be found in Table 3 in detail.

Therefore, the vessel's *SFOC* can be computed using either the actual engine curve or a regression model depending on whether a specific engine detail or just an estimation of the generic power limit was available. The final fuel consumption (*FC*) is then determined based on the aforementioned factors, which can be expressed as:

$$FC = SFOC\left(0.5\rho_{FW} S_W C_T V_S^2 + R_S + R_{BANK}\right) V_S \,/\, \eta_H \,/\, \eta_O \,/\, \eta_R \,/\, \eta_S \tag{11}$$

Table 2
Propulsive coefficients for twin propeller IWVs corresponding to varying water depths (data can be found in Kulczyk and Tabaczek (2014)).

$\frac{H}{T}$	w_E	t
≥3.0	Kristensen and Lützen (2012)	Schneekluth and Bertram (1998)
2.7	0.22	0.20
2.0	0.27	0.24
1.8	0.23	0.27
1.6	0.20	0.27
1.4	0.26	0.29
1.2	0.32	0.30

4. Results and discussion

This section presents example of simulation results, model verification study and investigation on the energy consumption of inland vessels. The purpose is to evaluate the applicability of the empirical methods within the ShipCLEAN-IWV model when applied to confined waterways and demonstrate its ability for dynamic monitoring of power demand and energy consumption. Section 4.1 and 4.2 show the verification of the resistance prediction module for single self-propelled vessel and pusher-barge systems, the results are compared to model test data under varying speed and water depth conditions from publicly literatures. Section 4.3 discusses the power estimation and how it is verified using full-scale measurement. The sensitivity analysis is presented in Section 4.4, which aims to investigate the impact of individual parameters on the entire vessel energy system. Besides, Section 4.5 presents an example study on the ship energy consumption under varying waterways data, vessel loading conditions (draft), and bank effect.

4.1. Single vessel: verification of resistance prediction

Fig. 6 shows the verification of the resistance prediction from the model developed in this study using the experimental data from Mucha et al. (2018). The figure indicates that in the case of deep water (when $\frac{H}{T} = \infty$), the estimated ship resistance R_T matched the experimental values perfectly. With decreasing water depth, a significant increase in resistance could be observed, and the comparison demonstrated that the overall prediction results from the developed model agreed well with the experimental data. Specifically, even for the shallowest case ($\frac{H}{T} = 1.2$), the model still worked at low speeds ($V < 0.9$ m/s). When the ship's speed increased, the resistance difference became larger, such difference might because the model did not consider a correction for the wave-making component in shallow water and thus the total resistance was underestimated. However, the shallowest case is relatively rare for inland ships during daily operation, and high-speed sailing should be avoided for safety when under keel clearance (UKC) is too small. In general, the developed model provided an accurate prediction resistance at different water depths despite being solely based on empirical formulas.

4.2. Pushed convoy: verification of resistance prediction

In addition to the single self-propelled inland vessel, the study also investigated resistance prediction for pushed convoys using the ship model test results from the literature; the hull geometry and detailed experimental data is available in Zentari et al. (2022). This experiment included three types of barge arrangements: Convoy 1:1, Convoy 2:1, and Convoy 2:2. The two digits represent the longitudinal and transverse arrangements of the barges, respectively, as seen in Fig. 7. The water depth, ship speed and total wetted surface area of each configuration

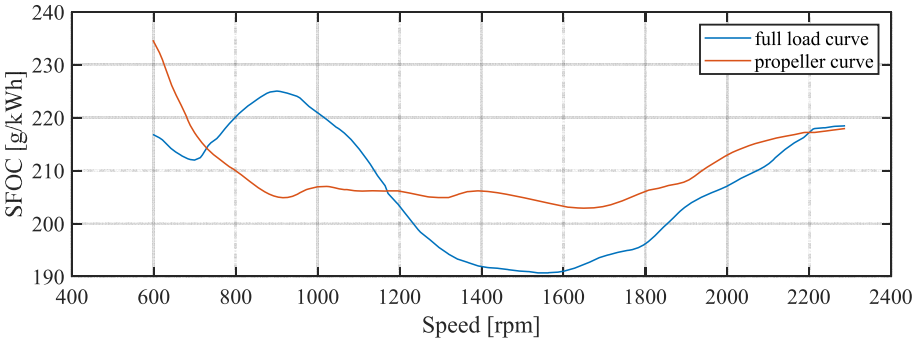

Fig. 5. SFOC curve of MAN D2862 marine diesel engine, reproduced from MAN Technical data sheet.

Table 3
SFOC prediction against P_S/P_{max} from Hidouche et al. (2015).

P_{max} [kW]	$X = P_S/P_{max}$[%]	$SFOC = f(X)$ [g/kW/h]	Error [%]
100–300	0–20	$398.89X^{-0.1987} + 8.945$	10
	20–100	$242.51 - 0.810X + 0.0065X^2$	7
300–500	0–20	$342.077X^{-0.1361}$	10
	20–100	$237.84 - 0.5957X + 0.0040X^2$	7
500–1000	0–20	$327.708X^{-0.1262} + 1.984$	15
	20–100	$230.192 - 0.4496X + 0.0033X^2$	10
1000–2000	0–20	$296.346X^{-0.0963} - 1.06$	10
	20–100	$236.786 - 0.7577X + 0.0064X^2$	10
2000–10000	0–20	$265.583X^{-0.0570} - 1.743$	7
	20–100	$240.204 - 0.9639X + 0.0064X^2$	5
>10,000	0–20	$218.92X^{-0.0570} - 1.4368$	–
	20–100	$198 - 0.7945X + 0.0053X^2$	5

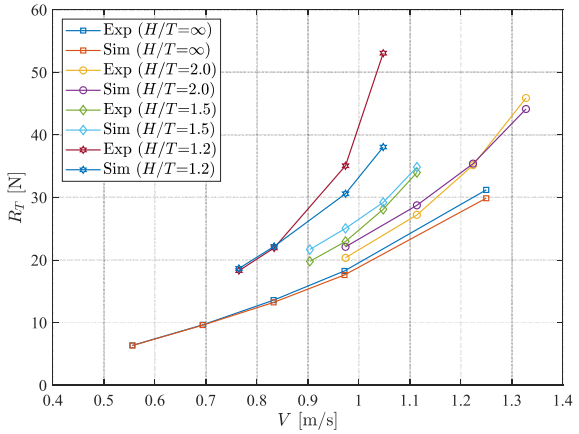

Fig. 6. Ship resistance prediction compared to model test data from Mucha et al. (2018).

were taken as the input, and the estimated resistance values are shown in Fig. 8. A comparison of the results showed that the model prediction fell within the range of experimental measurements for each pusher-barge configuration. Thus, the resistance prediction module could predict a generic ship's shallow water resistance even with very limited input. However, the results also reveals that the difference between the simulation and experimental values of resistance became noticeable when the convoy speed increased with decreasing water depth; this might be due to the interaction of the gap flow between the barges and the pusher, which become stronger when the ship's speed increases in shallow water. However, such a change in resistance could not be modelled with such limited input parameters, so this is out of scope for this paper. In general, the verification against the experimental data for single IWV and pusher-barge convoys indicated that the model performed well for a fast and accurate prediction of shallow water resistance.

4.3. Static and dynamic power prediction

The design of the propulsion units was based on the combination of a heavy-load propeller with a nozzle since it is mostly used in inland ships. The bladed section detail for the propeller was taken from the classical Ka-470 type. However, for the duct design, only a few airfoil types are available in OpenProp. Therefore, the duct was developed by incorporating the NACA 4315 mean line, which has a very similar sectional profile to the N19A nozzle. The desired thrust ratio for the propeller was 80% of the total thrust. The propeller geometry is shown in Fig. 9, showing a constant decrease in the thrust coefficient of the duct from the OpenProp design.

The power prediction was verified using full-scale data from the model test results in Friedhoff et al. (2019). The propulsive factors and demanded power for four inland vessels with different stern shapes and propeller configurations were investigated at three water depths (7.5 m, 5.0 m, and 3.5 m corresponding to full-scale). The results for two double crew vessels were selected for this study as their propeller diameters are identical; Table 4 lists the vessels' dimensions. The wetted surface area of each vessel was estimated based on the DTU and Holtrop–Mennen methods since these were not given in the literature. In addition, the mean value of the two vessels' results was selected (wetted surface area, effective and delivered power) to mitigate the impact of a specific hull shape, such as a flat stern or tunnelled aft. Because the aim was to perform a power prediction with limited parameters, the influence of the detailed hull shape could not be modelled with these inputs.

The power prediction at 7.5 m ($\frac{H}{T} = 2.68$) is shown in Fig. 10, in which the effective power P_E was computed using total resistance and ship speed, and the delivered power P_D was then computed using the hull coefficient η_H and an interpolation of η_O from the propeller open water curve according to sailing conditions. The proposed model provided a very good prediction of the ship's power demand at this water depth. When the vessel operated at 18 km/h, a difference in P_D between the simulation and experimental values could be observed, but it was still within 20%. Overall, the power prediction agreed well with tests under most conditions.

The results when the water level decreased to 5.0 m are shown in Fig. 11. The model was found to generate satisfactory predictions for ship speeds of less than 14 km/h. The magnitude of power differences became noticeable as the ship's speed increased further. This might be due to a stronger wave resistance when the ship sails in shallow water. Nevertheless, a correction for the wave induced part of the resistance was not included because a systematic method requires extensive model test experiments or CFD simulations, and it strongly depends on the vessel type, ship speed and water depth conditions (Du et al., 2020; Zeng

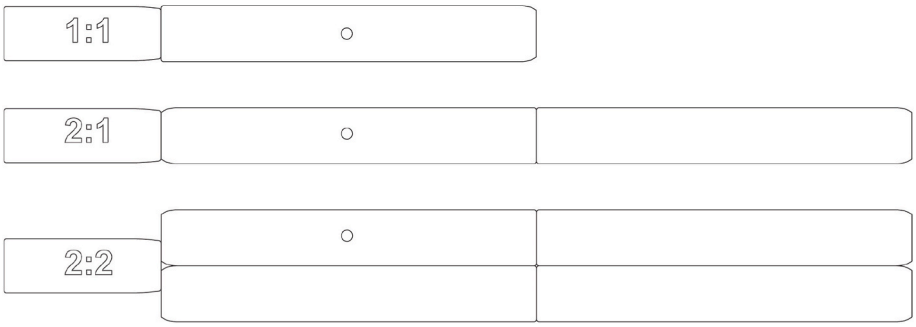

Fig. 7. The pusher-barge configuration in the experiment (Zentari et al., 2022).

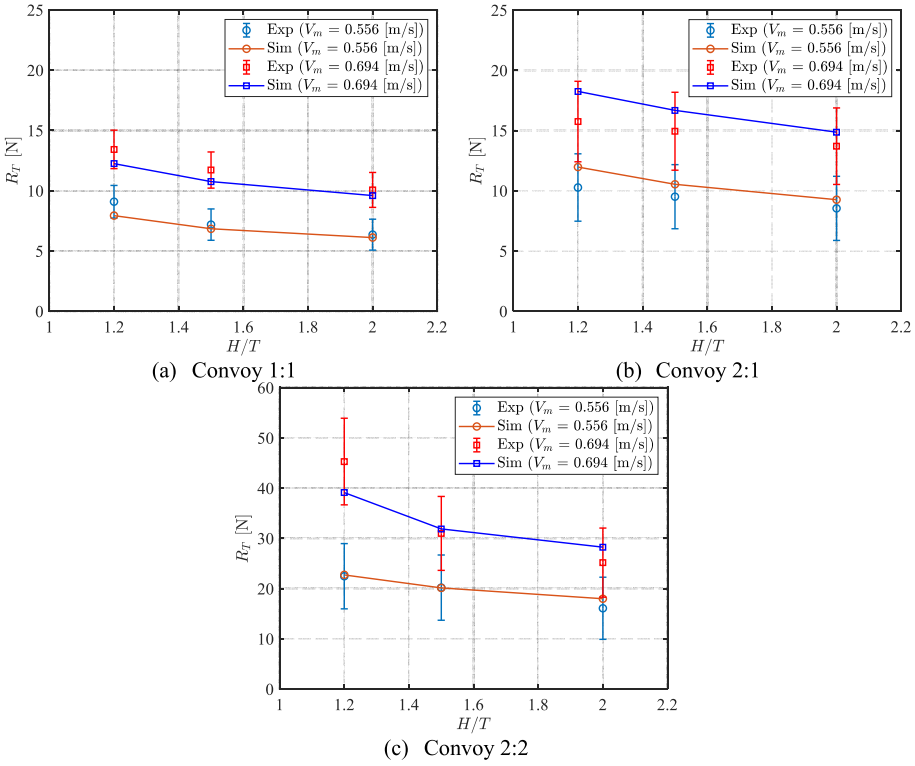

Fig. 8. Resistance prediction for pushed convoy for different barge arrangements using experimental data from Zentari et al. (2022).

et al., 2020). Similarly, as seen in Fig. 12, the proposed model underestimated the propulsion power at the shallowest water level. However, such a low under keel clearance made the calculation of wake field as well as thrust deduction extremely difficult, which contributed to high uncertainty in the estimation of delivered power. In general, the proposed model matched the generic operational conditions of inland vessels as it had good accuracy under most of the test conditions.

It also should be considered that the estimated wetted surface area might also have had some effect on the power prediction. An accurate wetted surface can easily be computed if the detailed hull shape is given, which can improve the resistance and power estimations.

4.4. Sensitivity analysis

A sensitivity analysis was performed to investigate the influence of the individual parameters on the energy performance of the entire ship. The goal is to determine the most important factors according to the magnitude change of the objective function with a small perturbation of each input. The objective function is defined as ship FC_{obj} here, and the sensitivity analysis focused on the gradient change of the FC, which can be described:

$$\frac{\partial FC_{obj}}{\partial \theta_i} \approx \frac{FC_{obj}(\theta_i + \varepsilon\theta_i) - FC_{obj}(\theta_i - \varepsilon\theta_i)}{2\varepsilon\theta_i} \tag{12}$$

where θ_i represents the target parameter for the entire ship's energy system and ε is a small perturbation, which is set according to the properties of each parameter. To mitigate the magnitude effect among the parameters, the partial derivative is normalised accordingly:

$$S_{\theta_i} = \lim_{\Delta\theta_i \to 0} \left(\frac{\Delta FC_{obj}/FC_{obj}}{\Delta\theta_i/\theta_i} \right) = \frac{\partial FC_{obj}}{\partial \theta_i} \frac{\theta_i}{FC_{obj}} \tag{13}$$

where S_{θ_i} is the sensitivity index for the FC variation with respect to the individual parameters. The vessel used in the sensitivity analysis has a length of 135 m, a beam of 11.45 m and a design draft of 3.2 m with a total displacement of 4450 t (90% loaded condition). These dimensions are typical for a large, self-propelled vessel (class type CEMT Vb) in European inland waterways (CEMT, 1992). The vessel is assumed to have twin screw ducted propellers with a diameter of 1.6 m, working at a target water level of 6.4 m ($\frac{H}{T} = 2.0$) and ship-bank distance of ($d = 2.0$

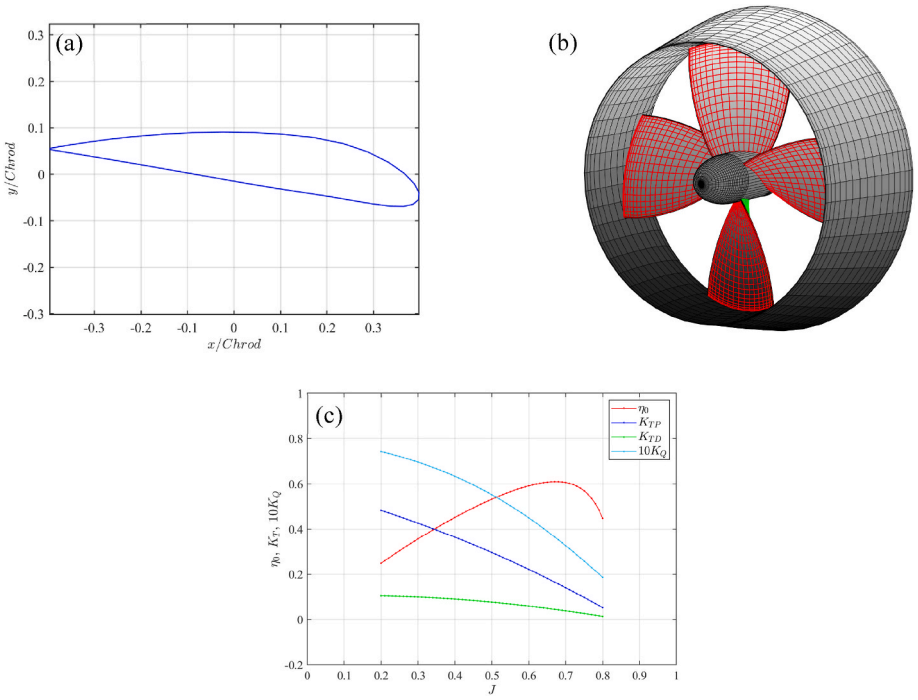

Fig. 9. Propeller geometry (a), (b); and open water curve (c).

Table 4
Hull dimensions of the studied vessels in Friedhoff et al. (2019).

Parameters	Unit	M2053	M2054
L	[m]	110	110
B	[m]	11.44	11.44
T	[m]	2.8	2.8
∇	[m^3]	3162	3129
c_B	[-]	0.90	0.89
n_{Prop}	[-]	2	2
D	[m]	1.6	1.6
S_W (estimated)	[m^2]	1799.27	1786.16

B) with a designed speed of 16 km/h, and the maximum engine limit is approximately 2000 kW. Table 5 lists the target parameters and corresponding initial values.

The results of the sensitivity analysis are shown in Fig. 13. The parameters which directly affect the *FC* calculation, namely S_W (θ_5), η_o (θ_{13}) and engine *SFOC* (θ_{14}), has the highest sensitivity index. Four parameters (θ_1 to θ_4) for the propeller and duct design were investigated, and the results shows that duct length is less sensitive than the other factors. In terms of resistance, c_f is the most sensitive, accounting for the largest proportion among the resistance components, yet a rather straightforward method is commonly used to estimate it with high accuracy. Besides, within the given bank distance, it is found that the R_{BANK} (represented by θ_{10}) become important as it causes more than 10% additional resistance, a small perturbation can have a certain impact on fuel consumption estimation. In addition, the form factor k and propulsive coefficients w_e and t should be considered carefully since they all had a sensitivity index above 0.25, which are considered as very important parameters.

4.5. Example study for energy consumption with waterway data

To investigate the ship's power demand and energy consumption during dynamic operation, water depth data for a reach of the Seine River with a total length of 153 km was selected from Linde (2017), and corresponding channel width data was acquired from the MERIT Hydro database (Yamazaki et al., 2019). The current speed U_C was computed according to two river discharge rates ($Q = 500$ m^3/s and $Q = 200$ m^3/s), and the waterway profile can be found in Figs. 14 and 15. The vessel described in section 4.4 was used for the simulation, in which four loading conditions (40%, 60%, 80% and fully loaded) were simulated using the waterway data mentioned above. The detailed dimensions for each loading rate are listed in Table 6.

All the simulations were conducted assuming that the vessel

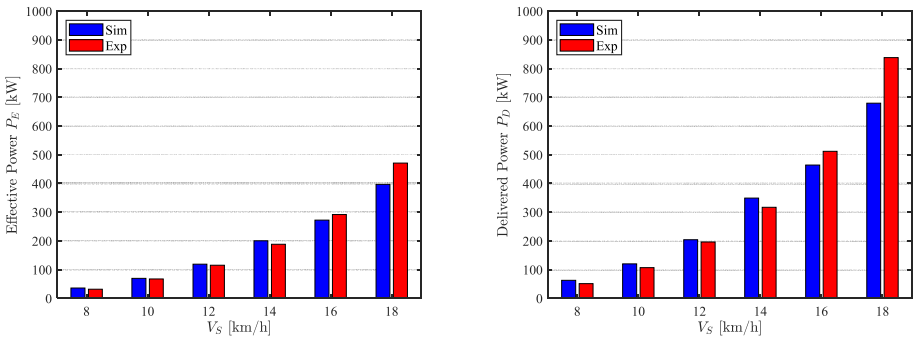

Fig. 10. Effective and delivered power prediction ($\frac{H}{T} = 2.68$).

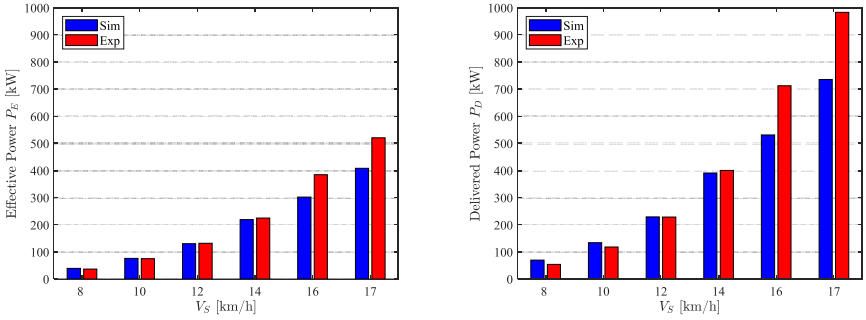

Fig. 11. Effective and delivered power prediction ($\frac{H}{T} = 1.78$).

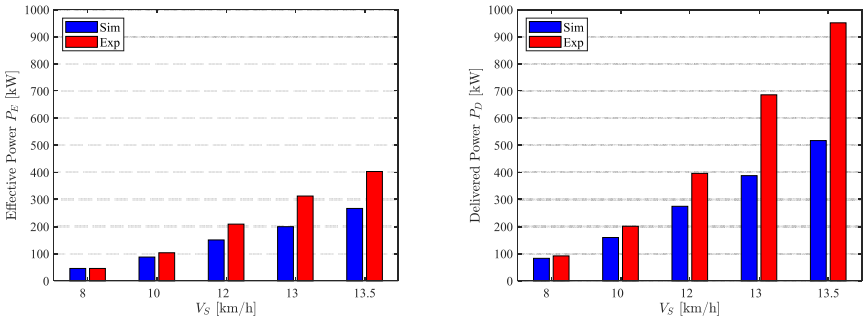

Fig. 12. Effective and delivered power prediction ($\frac{H}{T} = 1.25$).

Table 5
Parameters for the sensitivity analysis.

Id.	Parameters	Unit	Initial value	ε
θ_1	Propeller diameter (D)	[m]	1.60	0.10
θ_2	Propeller speed (rpm)	[n/min]	300	0.10
θ_3	Duct chord length (C)	[m]	0.80	0.10
θ_4	Propeller thrust ratio (τ)	[-]	0.80	0.10
θ_5	Wetted surface area (S_W)	[m^2]	2299.68	0.05
θ_6	Frictional resistance (C_F)	[-]	1.77e–3	0.01
θ_7	Form factor (k)	[-]	0.47	0.05
θ_8	Wave resistance (C_W)	[-]	3.94e–4	0.01
θ_9	Resistance due to squat (R_S /R_T)	[-]	0.027	0.01
θ_{10}	Resistance due to bank effect (R_{BANK}/ R_T)	[-]	0.138	0.01
θ_{11}	Effective wake (w_E)	[-]	0.40	0.10
θ_{12}	Thrust deduction (t)	[-]	0.30	0.10
θ_{13}	Open water efficiency (η_o)	[-]	0.45	0.10
θ_{14}	Engine *SFOC*	[g/kW/ h]	208.75	0.10

constantly operates at its design speed of $V_s = 16$ km/h. Fig. 16 shows the influence of the loading rate on power and energy consumption along the route. Compared to the average water depth, the shallowest water causes a 70% power increase at 40% loading, and up to a 100% increase in power under fully loaded conditions. The additional power results in a significant increase in the fuel consumption rate. In the plot of the bank effect, shown in Fig. 17, the dashed line does not show a huge difference from the solid one along most of the route, which means sailing at a distance 25% of the channel width to the bank has a limited influence on overall energy consumption. However, the figure also indicates that if the channel becomes narrow enough, the impact of the bank effect will increase instant fuel consumption by 30% (indicated by the blue box). The simulations for the bank effect on the accumulative fuel consumption under various loading conditions and river discharges are summarised in Fig. 18, where fuel consumption under 40% loading at the centre of the river was selected as the reference (red dashed line).

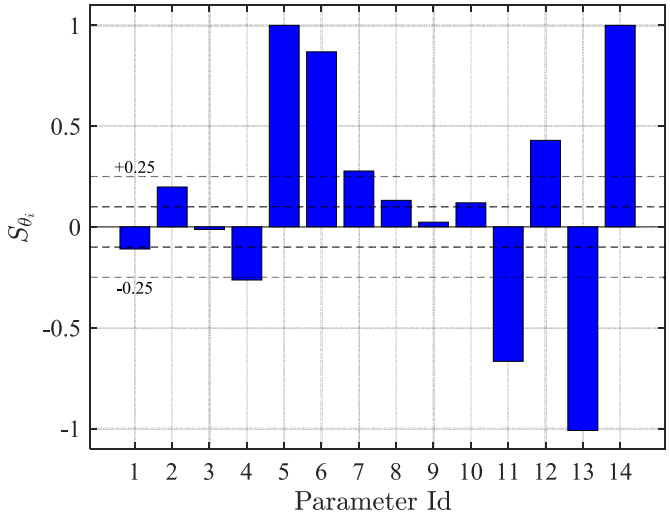

Fig. 13. Sensitivity analysis for the target parameters; the black and red dashed lines represent [–0.1 0.1] and [–0.25 0.25] sensitivity index ranges, respectively.

First, the ship draft influenced fuel consumption significantly: even though the fully loaded condition increased the wetted surface area S_w by 23% compared to the reference, the additional accumulative fuel consumption is even higher than 69%, as shown in the right column of Fig. 18 (a). Moreover, at a low discharge rate, the vessel consumes 6% more fuel oil compared to when $Q = 500$ m^3/s for upstream sailing at the same speed, even though the average depth H only decreased by 0.3 m (from 6.0 m to 5.7 m) and the current speed was considerably lower, as seen in Figs. 14 (c) and Fig. 15 (c). Therefore, during daily operation, either loading optimisation or speed optimisation including water depth data should be considered to minimise energy consumption.

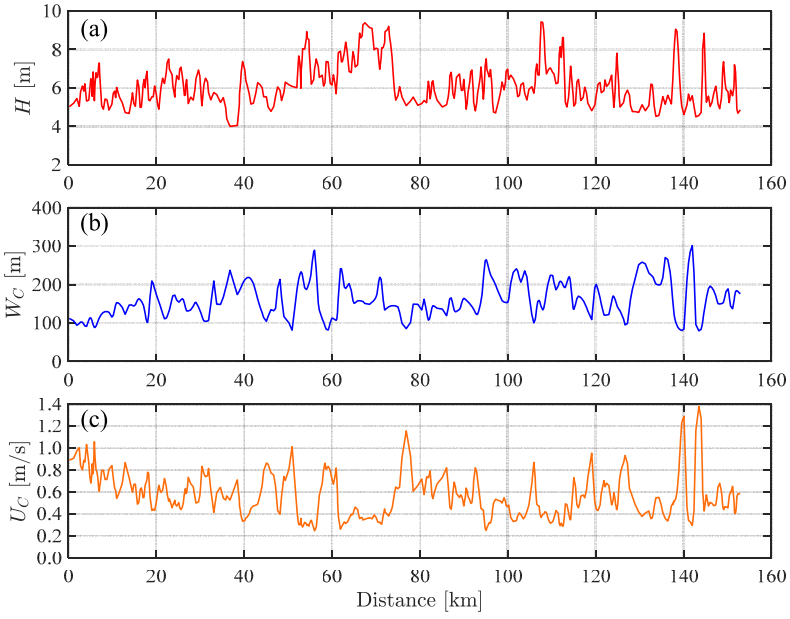

Fig. 14. Waterway profile of the selected reach ($Q = 500$ m^3/s).

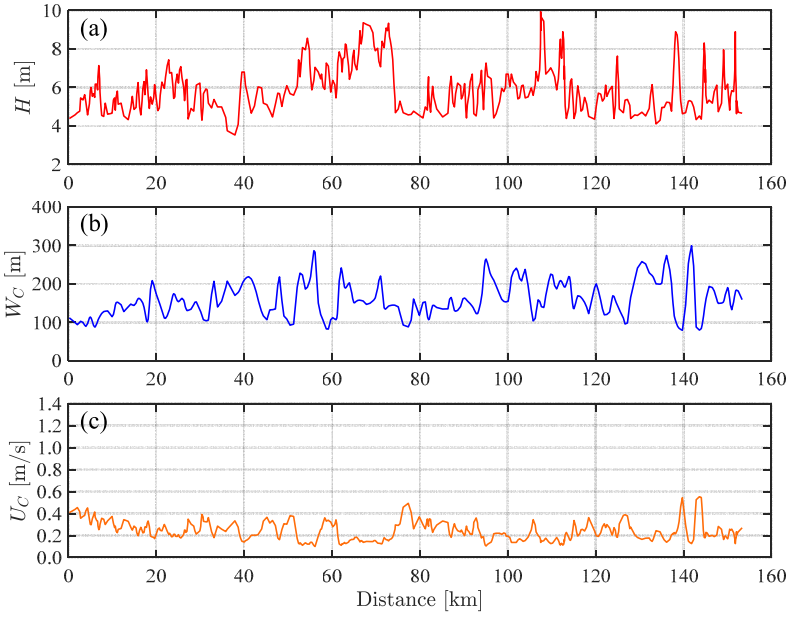

Fig. 15. Waterway profile of the selected reach (Q = 200 m^3/s).

Table 6
Vessel profile under different loading conditions.

Loading rate [-]	Displacement [t]	T [m]	S_W [m^2]
40%	2590	1.85	1859.01
60%	3390	2.40	2014.94
80%	4190	2.94	2169.12
100%	4990	3.50	2323.83

4.6. Discussion

This paper has developed an integrated model to evaluate the energy performance of IWVs. The modular-based model represents critical factors for the holistic propulsion system, and the overall goal was to provide a fast and accurate prediction of the demand propulsion power and energy consumption under dynamic inland waterway conditions.

The study investigated empirical methods with a specific focus on the ship's hydrodynamic properties in confined waterways. The accuracy of the resistance prediction module was verified using the model test data in the published literature. The results proves that the model could capture the variation of the total hull resistance in restricted water.

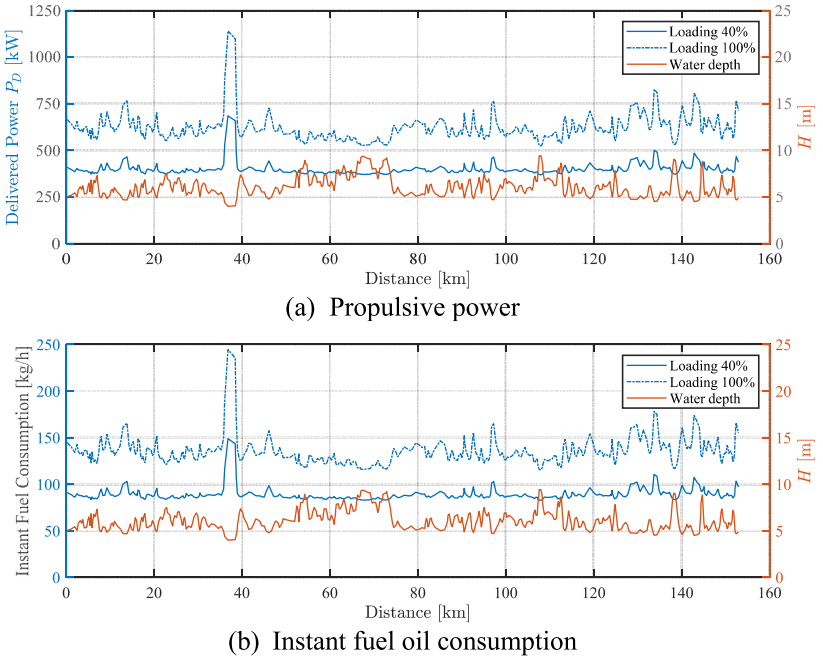

Fig. 16. The effect of loading rate on propulsive power and fuel consumption rate when the ship is sailing downstream at a constant desired speed of 16 km/h, under the discharge rate $Q = 500$ m^3/s.

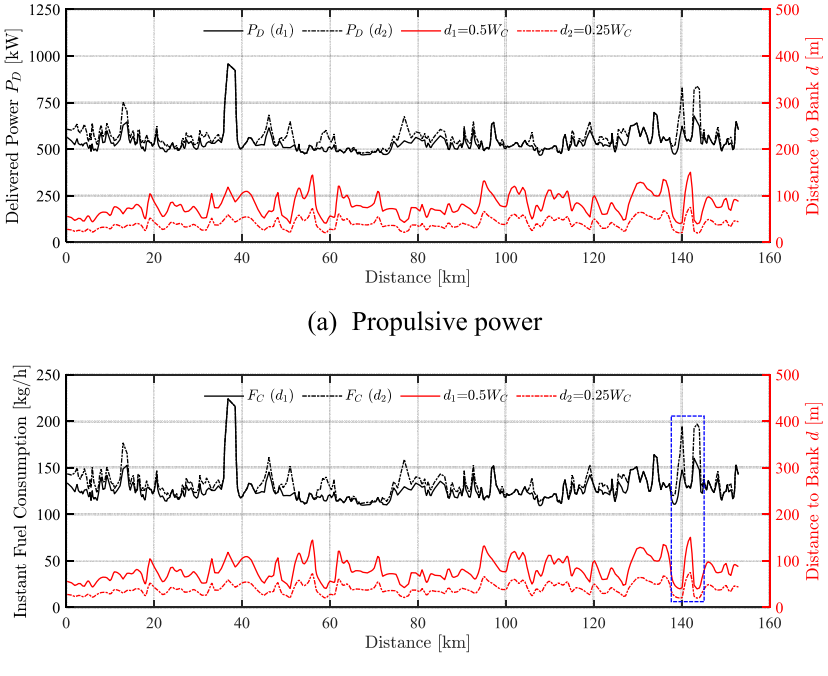

Fig. 17. The bank effect on power and instant fuel consumption when the vessel is sailing downstream under 80% loading.

However, the model might have underestimated the drag force when the ship's speed increases in extremely shallow water. Therefore, a correction in terms of wave resistance should be considered in future work using systematic CFD simulations.

The ducted propeller was designed to analyse the open water characteristics of the propulsion unit. Through this, the propeller open water efficiency could be derived according to the vessel's speed and thrust demand. The target is to give dynamic feedback on the propulsive factors with respect to the operational conditions (ship speed, water flow speed and geometry of the encountered waterways) instead of only using an estimated constant. A comparison with the full-scale experimental measurements indicates that the overall power estimation agreed with most of the operating conditions, and the model is capable of relatively accurate predictions using limited input parameters. In the future, the power prediction will be further validated for different ship types using experimental or even full-scale data.

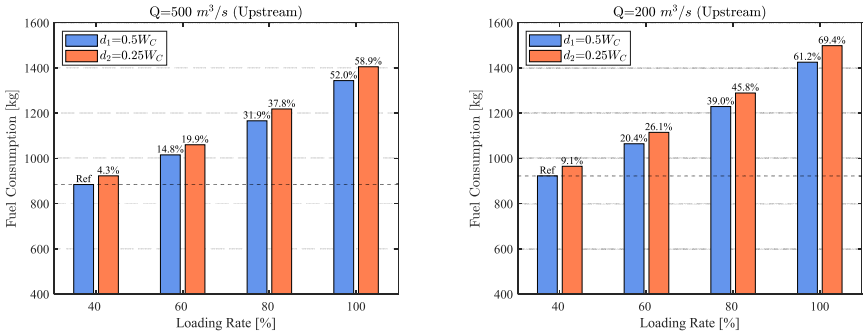

(a) Accumulated fuel consumption for upstream sailing.

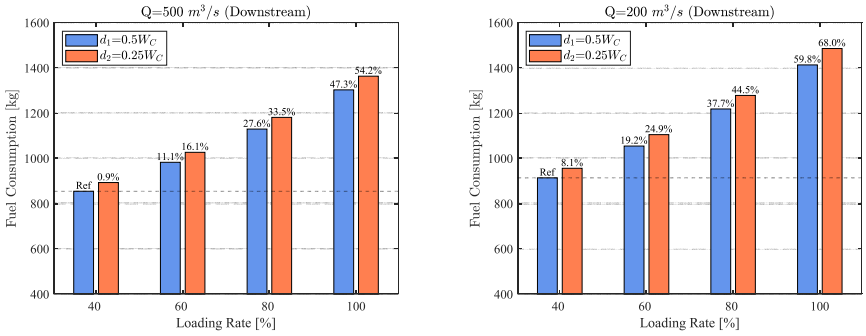

(b) Accumulated fuel consumption for downstream sailing.

Fig. 18. Prediction of the accumulative fuel oil consumption under various distances to the bank and vessel loading rates.

The example study investigated an inland vessel's accumulative energy consumption under different loading conditions. Hydraulic data from a small reach of the Seine River with a length of 153 km was selected from the published literature. Four loading conditions for the vessel, namely 40%, 60%, 80% and fully loaded, were studied under two river discharge rates (200 m^3/s and 500 m^3/s). The results suggests that the vessel's draft has the highest impact on the fuel consumption under a limited water depth. The fully loaded condition contributes more than 60% of the accumulative fuel consumption compared to low draft (40% loading), even though the wetted surface area only increases by less than 25%. Then, the bank effect was investigated for a closer ship–bank distance ($\frac{d}{W_C} = 0.25$); compared to water depth confinement, the bank effect has a lower overall impact on the power increase. However, it could still become significant if the fairway becomes narrow enough. However, this study only considering the constant speed operation of a single vessel. Varying speeds and pusher-barge convoy systems should be included with a more detailed hydrodynamic model in future work.

5. Conclusions

This paper has presented the development of a holistic energy performance model for inland vessels. The aim is to provide a fast and accurate prediction of the ship's resistance, power demanded and fuel oil consumption with limited input parameters. The model was developed based on an existing ship performance model, ShipCLEAN, which was designed for open water. The objective is, first, to improve the resistance prediction module and to enable it to consider the shallow water and bank effect in restricted waterways. Second, a ducted propeller design was conducted to capture the propeller efficiency and characteristics of conventional IWVs. Then, the engine model was applied to dynamic waterways data contains varying channel dimensions and ship positions to analyse the impact of operation and encountered waterway conditions on fuel oil consumption.

The resistance predictions were verified using published model test data for single self-propelled vessels and various pusher-barge configurations. The average model prediction error was approximately 5.8%, which showed good agreement with the experimental measurement. The greatest resistance difference occurred with the ship sailing at the highest speed under the shallowest water conditions ($\frac{H}{T} = 1.2$). Thus, the correction for wave making resistance in shallow water will be investigated in a future study. For the resistance prediction for the pusher-barge convoys, the overall model error was 8.7%. The increased discrepancies were likely due to the complex interaction at the gaps between the pusher and the individual barges. Although the error was slightly higher than the error for the single vessel, the predictions still fall within the range of experimental measurement. The power estimation indicated the model's capability under generic operating conditions, except for high-speed sailing in very shallow water, as the model underestimated the delivered power significantly. Finally, the study used a reach of Seine River data to analyse fuel oil consumption in dynamic inland waterways. The accumulated fuel consumption showed that the vessel–bank distance had a limited impact on total fuel consumption compared to the draft (loading rate) and water depth. However, sailing at 25% of the channel width still contributed 5% additional fuel oil consumption compared to sailing at the centreline of the studied waterway.

In conclusion, the model presented in the study is an effective method for estimating the power demand and fuel oil consumption of inland vessels. While the employed methods are primarily derived from previously published studies, their combination and integration into a single tool for predicting the energy consumption of inland water vessels, without the need for extensive testing or computations and without detailed knowledge of ship characteristics, represents a novel approach. This results in a unique ship performance model.

The combination of empirical methods showed its advantages in terms of computational efforts, accuracy, and robustness for generic vessel operating conditions. However, several shortcomings of this study should be addressed in future work. First, while the paper only addressed longitudinal hull force, the hydrodynamic behaviour of the vessel during steering (especially when the vessel makes a sharp turn in curved channels) is also important in terms of fuel oil consumption. The ship performance model should thus be extended with a three-degree of

freedom (3-DoF) manoeuvring model to gain a better understanding of the horizontal force and moment and their impact on energy consumption. Second, the correction for wave resistance in shallow water should be addressed to improve the model's accuracy. Third, the effect of ship generated waves is neglected due to model simplification; this effect can be significant when the vessel sails in very narrow channel, lock operation and crossing the bridges. However, to investigate wave patten is complicated and requires experiment or high-fidelity CFD simulation. In addition, the propeller performance should be investigated thoroughly, such as the influence of the duct geometry, inflow angle and axial speed since open water efficiency is critical to the power prediction. Finally, this study assumed the channel cross section to be rectangular (flat bottom with vertical walls); therefore, detailed bathymetry data and current field should be utilised to analyse the effect of channel geometry on the ship's routing selection and energy consumption in a future study.

CRediT authorship contribution statement

Chengqian Zhang: Conceptualization, Methodology, Formal analysis, Software, Data curation, Writing – original draft. **Jonas W. Ringsberg:** Conceptualization, Methodology, Supervision, Writing – review & editing, Project administration. **Fabian Thies:** Methodology, Supervision, Writing – review & editing.

Declaration of competing interest

The authors declare that they have no known competing financial interests or personal relationships that could have appeared to influence the work reported in this paper.

Data availability

Data will be made available on request.

Acknowledgements

This project has received funding from the European Union's EU Framework Programme for Research and Innovation Horizon 2020 under Grant Agreement No. 955768 (ETN AUTOBarge). Project website: https://etn-autobarge.eu/.

Appendix A. The virtual ship method

If the hull of the target inland vessel differs much from the references, e.g. the pusher barge train in Fig. 7, a virtual ship method is then applied (Zeng, 2019). The equivalent factor γ to compute the draft of the virtual ship is given as:

$$\gamma = -\frac{a_1}{(\log_{10}Re - 2)} + a_2 e^{-(H/T)^{0.06}} \tag{A.1}$$

where $a_1 = 5.7472C_B - 1.2989$ and $a_2 = 0.5738e^{1.8493C_B}$. It indicates that, the γ depends on hull fullness (C_B), Re and water depth ratio (H/T). With the factor γ, the frictional resistance of the target vessel is computed as:

$$C_F^* = C_{Fv}\frac{S_v}{S_W} + C_{Fb}\frac{S_b}{S_W} \tag{A.2}$$

where S_v is the vertical area ($S_v = 2L\gamma T$), S_b is the flat bottom ($S_b = LB$), C_{Fv} is the frictional resistance coefficient of vertical area, C_{Fb} is the frictional resistance coefficient of the flat bottom, the formulaes are given as:

$$\begin{aligned} C_{Fv} &= \frac{0.08468}{(\log_{10}Re - 1.631)^2} \\ C_{Fb} &= \frac{0.08169}{(\log_{10}Re - 1.717)^2}\left(1 + \frac{0.003998}{\log_{10}Re - 4.393}\left(\frac{D}{L}\right)^{-1.083}\right) \end{aligned} \tag{A.3}$$

where D is the distance between the flat bottom to channel bed.

Appendix B. Collected data for R_{BANK} estimation

Source	H/T [-]	d/B [-]	Fr_h [-]	R_T [N]	R_T (ref) [N]	ΔR_T [%]
Mucha et al. (2018)	1.2	3.537	0.474	17.55	17.44	0.63
	1.2	3.537	0.561	27.69	27.50	0.68
	1.2	3.537	0.605	36.48	36.10	1.05
	1.2	3.537	0.648	51.28	49.48	3.63
	1.2	2.358	0.474	18.40	17.44	5.50
	1.2	2.358	0.561	29.63	27.50	7.74
	1.2	2.358	0.605	39.32	36.10	8.91
	1.2	2.358	0.648	52.60	49.48	6.30
	1.2	1.179	0.474	21.16	17.44	21.3
	1.2	1.179	0.561	33.88	27.50	23.2
	1.2	1.179	0.605	43.86	36.10	21.5
	1.2	1.179	0.648	66.92	49.48	35.2
Du et al. (2020)	6.0	3.684	0.287	1.637	1.633	0.23
	6.0	3.684	0.439	3.541	3.535	0.18
	6.0	3.684	0.515	5.052	5.002	1.05
	6.0	3.684	0.594	6.861	6.820	0.60

(continued on next page)

(*continued*)

Source	H/T [-]	d/B [-]	Fr_h [-]	R_T [N]	R_T (ref) [N]	ΔR_T [%]
	6.0	2.105	0.287	1.786	1.633	9.38
	6.0	2.105	0.439	3.921	3.535	10.91
	6.0	2.105	0.515	5.381	5.002	7.62
	6.0	2.105	0.594	7.645	6.820	12.09
	6.0	1.316	0.287	1.948	1.633	19.28
	6.0	1.316	0.439	4.551	3.535	28.73
	6.0	1.316	0.515	6.558	5.002	31.15
	6.0	1.316	0.594	9.468	6.820	38.82
Linde et al. (2017)	5.0	2.5	0.181	1.129	1.078	4.73
	5.0	2.5	0.271	2.354	2.201	6.95
	5.0	2.0	0.181	1.161	1.078	7.69
	5.0	2.0	0.271	2.427	2.201	10.26
	5.0	1.5	0.181	1.215	1.078	12.69
	5.0	1.5	0.271	2.560	2.201	16.31
	5.0	1.0	0.181	1.325	1.078	22.91
	5.0	1.0	0.271	2.806	2.201	27.50

References

Aztjushkov, L., 1968. Wall Effect Correction for Shallow Water Model Tests, vol. 85. North East Coast Institution of Engineers and Shipbuilders, Bolbec Hall, Great Britain, Transactions, Russia. No. 2, Leningrad Shipbuilding Institute.

Bui, K.Q., Perera, L.P., 2021. Advanced data analytics for ship performance monitoring under localized operational conditions. Ocean Eng. 235.

Calleya, J.N., 2014. Ship Design Decision Support for a Carbon Dioxide Constrained Future. Doctoral Thesis. UCL Press, London.

Campbell, R., Terziev, M., Tezdogan, T., Incecik, A., 2022. Computational fluid dynamics predictions of draught and trim variations on ship resistance in confined waters. Appl. Ocean Res. 126, 103301.

CEMT, 1992. Resolution No.92/2: on new classification of inland waterways. Tech. Rep. 92. European Conference of Ministers of Transport.

Du, P., Ouahsine, A., Sergent, P., Hoarau, Y., Hu, H., 2021. Investigation on resistance, squat and ship-generated waves of inland convoy passing bridge piers in a confined waterway. J. Mar. Sci. Eng. 9 (10), 1125.

Du, P., Ouahsine, A., Sergent, P., Hu, H., 2020. Resistance and wave characterizations of inland vessels in the fully-confined waterway. Ocean Eng. 210, 107580.

Epps, B., Chalfant, J., Kimball, R., Techet, A., Flood, K., Chryssostomidis, C., 2009. OpenProp: an open-source parametric design and analysis tool for propellers. In: Proceedings of the 2009 Grand Challenges in Modeling & Simulation Conf., pp. 104–111.

European Commission, 2020. MSCA-ETN-AUTOBarge. https://etn-autobarge.eu/ (Accessed 11 September 2023).

Eurostat, 2022. 77% of inland freight transported by road in 2020. https://ec.europa.eu/eurostat/en/web/products-eurostat-news/-/ddn-20220425-2. (Accessed 15 August 2023).

Eurostat, 2023. Quarterly Greenhouse Gas Emissions in the EU. https://ec.europa.eu/eurostat/statistics-explained/index.php?title=Quarterly_greenhouse_gas_emissions_in_the_EU#Emissions_by_economic_activity. (Accessed 15 August 2023).

Friedhoff, B., Hoyer, K., List, S., Tenzer, M., 2019. Investigation of the nominal and effective propeller inflow for a family of inland waterway vessels. Ocean Eng. 187.

Geerts, S., Verwerft, B., Vantorre, M., Van Rompuy, F., 2010. Improving the efficiency of small inland vessels. In: Proceedings of the 7th European Inland Waterway Navigation Conference. Budapest Univ. of Technology and Economics, Budapest, Hungary.

Gupta, P., Rasheed, A., Steen, S., 2022. Ship performance monitoring using machine-learning. Ocean Eng. 254.

Harvald, S.A., 1992. Resistance and Propulsion of Ships. John Wiley & Sons.

Hidouche, S., Guitteyn, M., Linde, F., Sergent, P., 2015. Ships propulsion: estimation of specific fuel consumption based on power load factor ratio. In: Proceedings of Hydrodynamics and Simulation Applied to Inland Waterways and Port Approaches.

Hooft, J. P., 1977. The influence of nautical requirements on the dimensions and layout of entrance channels and harbours., Proc. International Course Modern Dredging, The Hague, Netherlands.

Hu, Z.H., Jing, Y.X., Hu, Q.Y., Sen, S., Zhou, T.R., Osman, M.T., 2019. Prediction of fuel consumption for enroute ship based on machine learning. IEEE Access 7, 119497–119505.

Huang, L.F., Li, Z.Y., Ryan, C., Ringsberg, J.W., Pena, B., Li, M.H., Ding, L., Thomas, G., 2021. Ship resistance when operating in floating ice floes: derivation, validation, and application of an empirical equation. Mar. Struct. 79.

Islam, H., Soares, C.G., Liu, J., Wang, X., 2021. Propulsion power prediction for an inland container vessel in open and restricted channel from model and full-scale simulations. Ocean Eng. 229.

Karagiannidis, P., Themelis, N., 2021. Data-driven modelling of ship propulsion and the effect of data pre-processing on the prediction of ship fuel consumption and speed loss. Ocean Eng. 222.

Karpov, A., 1946. Calculation of Ship Resistance in Restricted Waters, vol. 2. TRUDY GII. T. IV (in Russian).

Kristensen, H.O., Lützen, M., 2012. Prediction of resistance and propulsion power of ships. Clean Shipp. Currents 1 (6), 1–52.

Kulczyk, J., 1995. Propeller-hull interaction in inland navigation vessel. Trans. Built Environ. 11, 73–89.

Kulczyk, J., Tabaczek, T., 2014. Coefficients of propeller-hull interaction in propulsion system of inland waterway vessels with stern tunnels. TransNav: Int. J. Mar. Navig. Saf. Sea Transp. 8 (3), 377–384.

Landweber, L., 1939. Tests of a Model in Restricted Channels. David Taylor Model Basin, Washington DC.

Lang, X., Wu, D., Mao, W.G., 2022. Comparison of supervised machine learning methods to predict ship propulsion power at sea. Ocean Eng. 245.

Lataire, E., Vantorre, M., Eloot, K., 2009. Systematic Model Tests on Ship-Bank Interaction Effects, International Conference on Ship Manoeuvring in Shallow and Confined Water: Bank Effects. London Royal Institution of Naval Architects, pp. 9–22.

Linde, F., 2017. 3D modelling of ship resistance in restricted waterways and application to an inland eco-driving prototype. Doctoral Thesis. Université de Technologie de Compiègne, France.

Linde, F., Ouahsine, A., Huybrechts, N., Sergent, P., 2017. Three-dimensional numerical simulation of ship resistance in restricted waterways: effect of ship sinkage and channel restriction. J. Waterw. Port, Coast. Ocean Eng. 143 (1).

Lu, R.H., Turan, O., Boulougouris, E., Banks, C., Incecik, A., 2015. A semi-empirical ship operational performance prediction model for voyage optimization towards energy efficient shipping. Ocean Eng. 110, 18–28.

MAN-D2862 technical data sheet. https://www.tonissi.com/wp-content/uploads/2017/06/data-d2862le446-v12-1400-epa-t3.pdf. (Accessed 15 August 2023).

Millward, A., 1989. The effect of water depth on hull form factor. Int. Shipbuild. Prog. 36 (407).

Mucha, P., el Moctar, O., Dettmann, T., Tenzer, M., 2017. Inland waterway ship test case for resistance and propulsion prediction in shallow water. Ship Technol. Res. 64 (2), 106–113.

Mucha, P., el Moctar, O., Dettmann, T., Tenzer, M., 2018. An experimental study on the effect of confined water on resistance and propulsion of an inland waterway ship. Ocean Eng. 167, 11–22.

Parkes, A.I., Sobey, A.J., Hudson, D.A., 2018. Physics-based shaft power prediction for large merchant ships using neural networks. Ocean Eng. 166, 92–104.

Pompée, P.-J., 2015. About modelling inland vessels resistance and propulsion and interaction vessel-waterway. key parameters driving restricted/shallow water effects. In: Proceeding of Smart Rivers 2015. The World Association for Waterborne Transport Infrastructure (PIANC) Buenos.

Raven, H., 2012. A computational study of shallow-water effects on ship viscous resistance. In: Proceedings of the 29th Symposium on Naval Hydrodynamics. Gothenburg, Sweden.

Raven, H., 2016. A new correction procedure for shallow-water effects in ship speed trials. In: Proceedings of the 2016 PRADS Conference. Copenhagen.

Rotteveel, E., Hekkenberg, R., van der Ploeg, A., 2017. Inland ship stern optimization in shallow water. Ocean Eng. 141, 555–569.

Schlichting, O., 1934. Ship resistance in water of limited depth-resistance of sea-going vessels in shallow water. Jahrbuch der STG 35, 127–148.

Schneekluth, H., Bertram, V., 1998. Ship Design for Efficiency and Economy. Butterworth-Heinemann, Oxford.

Tillig, F., 2020. Simulation Model of a Ship's Energy Performance and Transportation Costs. Doctoral Thesis. Chalmers Tekniska Hogskola, Sweden.

Tillig, F., Ringsberg, J., Mao, W., Ramne, B., 2017. A generic energy systems model for efficient ship design and operation. Proc. IME M J. Eng. Marit. Environ. 231 (2), 649–666.

Tillig, F., Ringsberg, J.W., 2019. A 4 DOF simulation model developed for fuel consumption prediction of ships at sea. Ships Offshore Struct. 14 (Suppl. 1), 112–120.

Tillig, F., Ringsberg, J.W., 2020. Design, operation and analysis of wind-assisted cargo ships. Ocean Eng. 211, 107603.
Tillig, F., Ringsberg, J.W., Mao, W., Ramne, B., 2018. Analysis of uncertainties in the prediction of ships' fuel consumption–from early design to operation conditions. Ships Offshore Struct. 13 (Suppl. 1), 13–24.
Yamazaki, D., Ikeshima, D., Sosa, J., Bates, P.D., Allen, G.H., Pavelsky, T.M., 2019. MERIT Hydro: a high-resolution global hydrography map based on latest topography dataset. Water Resour. Res. 55 (6), 5053–5073.
Yuan, Z., Liu, J., Zhang, Q., Liu, Y., Yuan, Y., Li, Z., 2021. Prediction and optimisation of fuel consumption for inland ships considering real-time status and environmental factors. Ocean Eng. 221.
Zeng, Q., 2019. A Method to Improve the Prediction of Ship Resistance in Shallow Water. Delft University of Technology, Netherland.
Zeng, Q., Hekkenberg, R., Thill, C., Hopman, H., 2020. Scale effects on the wave-making resistance of ships sailing in shallow water. Ocean Eng. 212, 107654.
Zeng, Q., Thill, C., Hekkenberg, R., 2018. A benchmark test of ship resistance in extremely shallow water. In: Progress in Maritime Technology and Engineering – Guedes Soares & Santos. CRC Press, pp. 221–229.
Zeng, Q.S., Hekkenberg, R., Thill, C., 2019. On the viscous resistance of ships sailing in shallow water. Ocean Eng. 190.
Zentari, L., el Mocta, O., Lassen, J., Hallmann, R., Schellin, T.E., 2022. Experimental and numerical investigation of shallow water effects on resistance and propulsion of coupled pusher-barge convoys. Appl. Ocean Res. 121.
Zou, L., Larsson, L., 2013. Computational fluid dynamics (CFD) prediction of bank effects including verification and validation. J. Mar. Sci. Technol. 18 (3), 310–323.